Immune-deficient nude mice, which are highly susceptible to tumorigenicity, were also used in this experiment.

MATERIALS AND METHODS

Animals

Five-week-old female BALB/cJ and SJL/J, and five-week-old male BALB/cAnCrj-nu mice were purchased from Charles River (Japan) and maintained in the animal center according to the NIHS animal welfare guidelines. All mice were fed standard pellet diets and water *ad libitum* before and after PLLA implantation.

Implantation of PLLA

PLLA was obtained from Shimadzu Co. Ltd. as uniform sheets. The implants (size, 20 × 10 × 1 mm^3; Mw, 200,000) were sterilized using ethylene oxide gas prior to use. Sodium pentobarbital (4 mg/kg) was intraperitoneally administered to the mice. The dorsal skin was shaved and scrubbed with 70% alcohol. Using an aseptic technique, an incision of about 2 cm was made; a subcutaneous pocket was formed by blunt dissection away from the incision, and one piece of PLLA was placed in the pocket. The incision was closed with silk sutures. In both strains, controls were obtained by sham operation and subsequent subcutaneous pocket formation. Following surgery, the mice were housed in individual cages. After 10 months, mice from the implanted group were killed, implanted materials were excised, and subcutaneous tissues from the adjacent sites were collected for culture. At the same time, subcutaneous tissues were removed from the sites in the sham-operated controls that correlated with the implant sites. Similar experiments were also performed 1 month after PLLA implantation.[22]

Cell culture of subcutaneous tissues

The subcutaneous tissues were maintained in minimum essential medium (MEM) supplemented with 10% FBS in a 5% CO_2 atmosphere at 37°C.

Giemsa staining

When cells reached confluence in tissue culture dishes, they were fixed and stained with Giemsa solution. Cell morphology was determined under an inverted light microscope.

Western blot analysis

When cells had grown confluent in 60-mm tissue culture dishes, all cells were lysed directly in 100 μL 2% sodium dodecyl sulfate (SDS) gel loading buffer (50 m*M* Tris-HCl, pH 6.8, 100 m*M* 2-mercaptoethanol, 2% SDS, 0.1% bromophenol blue, and 10% glycerol). The protein concentration of the cleared lysate was measured using a micro-plate BCA protein assay (Pierce, Rockford, IL). Equivalent protein samples were analyzed by 7.5% SDS-polyacrylamide gel electrophoresis. The proteins were transferred to Hybond-ECL nitrocellulose membranes (Amersham Pharmacia Biotech UK, Buckinghamshire, UK), and Cx 43 protein was detected by anti-Cx 43 polyclonal antibodies (ZYMED Laboratories, San Francisco, CA). The membrane was soaked with Block Ace (Yukijirushi Nyugyo, Sapporo, Japan), reacted with the anti-Cx 43 polyclonal antibodies for 1 h, and after washes with phosphate-buffered saline (PBS) containing 0.1% Tween20, reacted with the secondary anti-rabbit IgG antibody conjugated with horseradish peroxidase for 1 h. After several washes with PBS-Tween20, the membrane was detected with the ECL detection system (Amersham Pharmacia Biotech UK).

Scrape-loading and dye transfer assay

The scrape-loading and dye transfer (SLDT) technique was performed by the method of El-Fouly et al.[24] Confluent monolayer cells in 35-mm culture dishes were used. After rinsing with Ca^{2+}, Mg^{2+} PBS(+), cell dishes were loaded with 0.1% Lucifer Yellow (Molecular Probes, Eugene, OR) in PBS(+) solution and were scraped immediately with a sharp blade. After incubation for 5 min at 37°C, cells were washed three times with PBS(+), and the extent of dye transfer was monitored using a fluorescence microscope equipped with a type UFX-DXII CCD camera and a super high-pressure mercury lamp power supply (Nikon, Tokyo, Japan).

Enzyme-linked immunosorbent assay

Cells were seeded onto 60-mm dishes. The conditioned medium was collected after centrifugation at 1000 rpm for 2 min. The TGF-β1 levels of the media were measured with commercially available enzyme linked immunosorbent assay (ELISA) kits (R&D Systems, Minneapolis, MN).

DNA microarray analysis

At least 10^7 cells were harvested and frozen in liquid nitrogen. Total RNA was extracted, purified, and assessed for yield and purity, and cDNA probes were synthesized with the Atlas™ Pure Total RNA Labeling System (Clontech) according to the manufacturer's instructions. Hybridization of the ^{33}P-labeled probes to the Atlas Array of Mouse Cancer 1.2 k Array (Clontec 7858–1), on which 1176 cDNAs

of cancer-related genes were spotted, was performed with Atlas™ cDNA Expression Arrays according to the manufacturer's instructions. The phosphor images of hybridized arrays were analyzed with AtlasImage™ (Clontech). Genes that were up- or downregulated more than fivefold relative to the negative controls are discussed.

Determination of tumorigenicity in nude mice

Cultured cells were harvested by trypsinization, and 2×10^6 washed cells suspended in 0.2 mL of PBS were inoculated at a single subcutaneous site into 6–8-week-old nude mice. All mice were examined regularly for the development of tumor.

Soft agar assay

Approximately 100,000 cells per well from each clone were seeded in 2 mL of 0.3% soft agar in culture medium on a solidified basal layer in 6-well tissue culture plates. The plates were cultured for 4 weeks and then stained with *p*-iodotetrazolium violet for 48 h before counting.

Statistical analysis

Student *t* tests were used to assess whether differences observed between the implanted and control samples were statically significant. For comparison of groups of means, one-way analysis of variance was carried out. When significant differences were found, Tukey's pairwise comparisons were used to investigate the nature of the difference. The confidence level was set at 95% for all tests. Statistical significance was accepted at $p < 0.05$. Values were presented as the mean ± SD.

RESULTS

Giemsa staining

Cells with different morphologies formed a slightly crisscrossed pattern in the BALB/cJ control group, whereas cells in the implanted groups of BALB/cJ showed a markedly crisscrossed pattern. The cells were extensively piled up, which decreased contact inhibition, under inverted light microscopy observation and Giemsa staining [Fig. 1(A,B)]. In contrast, the cells of the SJL/J group formed a parallel, flat, confluent monolayer that maintained contact inhibition [Fig. 1(C,D)].

Western blot analysis

We examined the protein expression of the connexin 43 gene and found that the total protein level was significantly decreased in PLLA-implanted BALB/cJ mice when compared with that in BALB/cJ controls (Fig. 2). However, protein expression was decreased in both control and PLLA-implanted groups in SJL/J mice (Fig. 2).

SLDT assay

The SLDT assay was used to assess functional GJIC. GJIC was significantly inhibited in PLLA-implanted BALB/cJ mice when compared with that in BALB/cJ controls (Fig. 3). A significant difference was also observed between the two strains of mice in that the GJIC was lower in SJL/J than in BALB/cJ group (Fig. 3).

ELISA

The secretion of TGF-β1 was significantly increased in PLLA-implanted BALB/cJ subcutaneous tissues in comparison with that from BALB/cJ control mice. On the contrary, secretion of TGF-β1 tended to decrease in the SJL/J implanted mice when compared with that in SJL/J control mice (Fig. 4).

DNA microarray analysis of the four kinds of cells

Expression of the major ECM [fibronectin 1, procollagen VIIIα 1, and osteopontin precursor (OPN)] proteins [Fig. 5(A–C)], insulin-like growth factor binding protein (IGFBP) 3 [Fig. 5(D)], and cysteine-rich intestinal protein 2 (CRIP 2) [Fig. 5(E)] were increased in the PLLA-implanted BALB/cJ mouse cells when compared with that in BALB/cJ control mouse cells. No such difference was observed between SJL/J implanted and control mouse cells.

Tumorigenicity in nude mice

No tumor was formed in PBS(−) injected nude mice [Fig. 6(A)]. Rapid growth of large tumors was observed in nude mice within 2 weeks of injection of cultured cells from PLLA-implanted BALB/cJ mice [Fig. 6(B,C,E,F)]. Nude mice injected with HeLa cells, which served as positive controls, showed slower growth of tumor 4 weeks after cell injection [Fig. 6(D,G)].

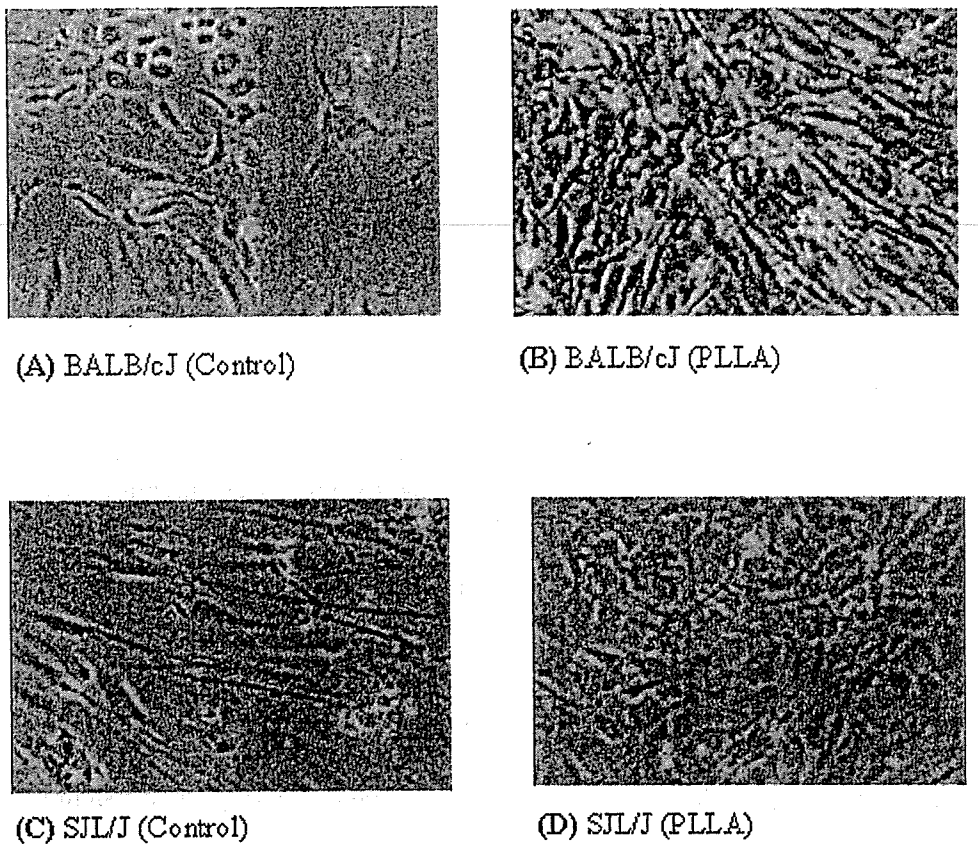

Figure 1. Mouse cell morphology. Three each of both implanted mice and sham-operated controls were killed after 10 months. Results shown are representative of two independent experiments. Inverted light microscopic appearance (magnification ×100) of (A) BALB/cJ (control), (B) BALB/cJ (PLLA), (C) SJL/J (control), and (D) SJL/J (PLLA). [Color figure can be viewed in the online issue, which is available at www.interscience.wiley.com.]

Soft agar assay

These tumor cells did not form a colony in soft agar (data not shown), although HeLa cells did form colonies in soft agar.

Histopathology

Tumor cells from nude mice injected with PLLA-implanted BALB/cJ mouse cells showed monophasic

Figure 2. Expression of Cx 43 protein by Western blot analysis. Three each of both implanted mice and sham-operated controls were killed after 10 months. Results shown are representative of two independent experiments. Total protein expression was significantly decreased in PLLA-implanted BALB/cJ mice when compared with that in the control. However, protein expression was decreased in both control and PLLA-implanted groups in SJL/J mice.

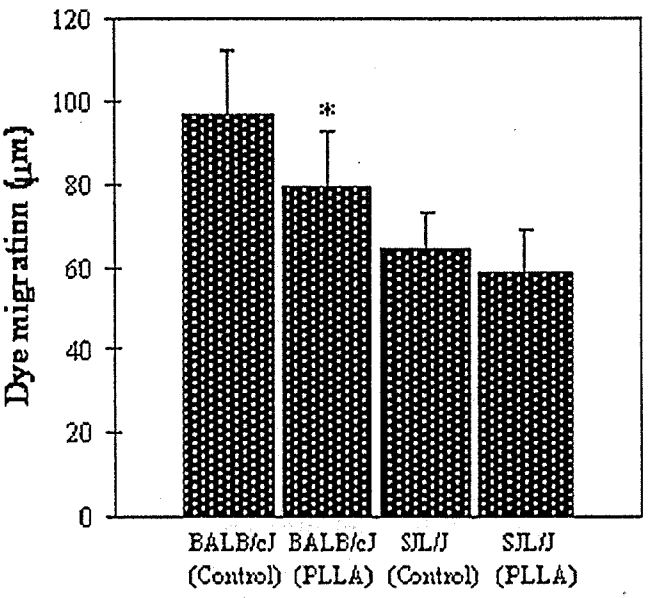

Figure 3. Statistical analysis of SLDT assay. Three each of both implanted mice and sham-operated controls were killed after 10 months. Results shown are representative of two independent experiments. GJIC was found to be significantly inhibited in PLLA-implanted BALB/cJ mice cells when compared with that in BALB/cJ controls. *$p < 0.05$.

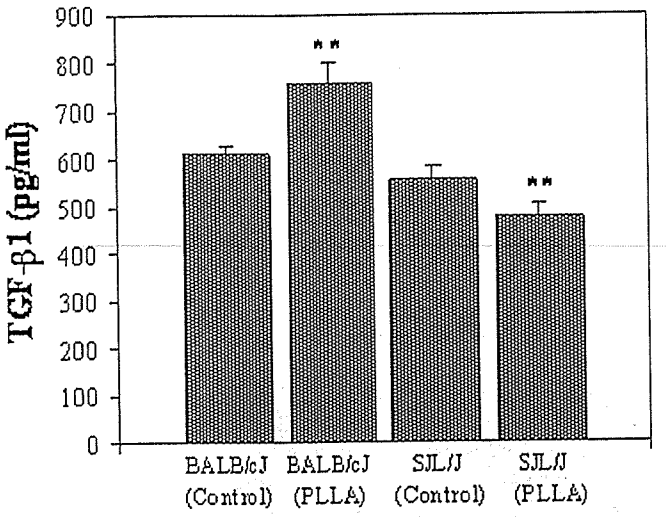

Figure 4. Statistical analysis of TGF-β1 cytokine assay by ELISA. Three each of both implanted mice and sham-operated controls were killed after 10 months. Results shown are representative of two independent experiments. Secretion of TGF-β1 level was significantly increased in PLLA-implanted BALB/cJ mice when compared with that in BALB/cJ controls. On the contrary, in the SJL/J mice, secretion of TGF-β1 tended to decrease in PLLA-implanted mice when compared with that in control mice. $^{**}p < 0.01$.

fibrous synovial sarcoma on H&E and keratin AE1/AE3 staining. Tumor cells with a staghorn pattern [Fig. 7(A)] and a herringbone pattern were identified [Fig. 7(B,C)].

DISCUSSION

Polylactides are bioabsorbable polyesters with wide range of clinical applications. Because it degrades slowly, PLLA has been used as a biomaterial for surgical devices such as bone plates, pins, and screws. It has been reported in different studies that polyetherurethane, nonabsorbable polyethylene, and PLLA produced tumors in rats.[9,10,25–27] Parallel to these studies, here cells with different morphologies formed a crisscross pattern, which thus decreased the contact inhibition in the PLLA-implanted BALB/cJ group [Fig. 1(B)]. We examined the protein expression of Cx 43 to evaluate the actual cause and found that the total level of protein expression was significantly decreased in the PLLA-implanted groups when compared with that in the controls (Fig. 2). In contrast, Cx 43 protein expression was decreased in both control

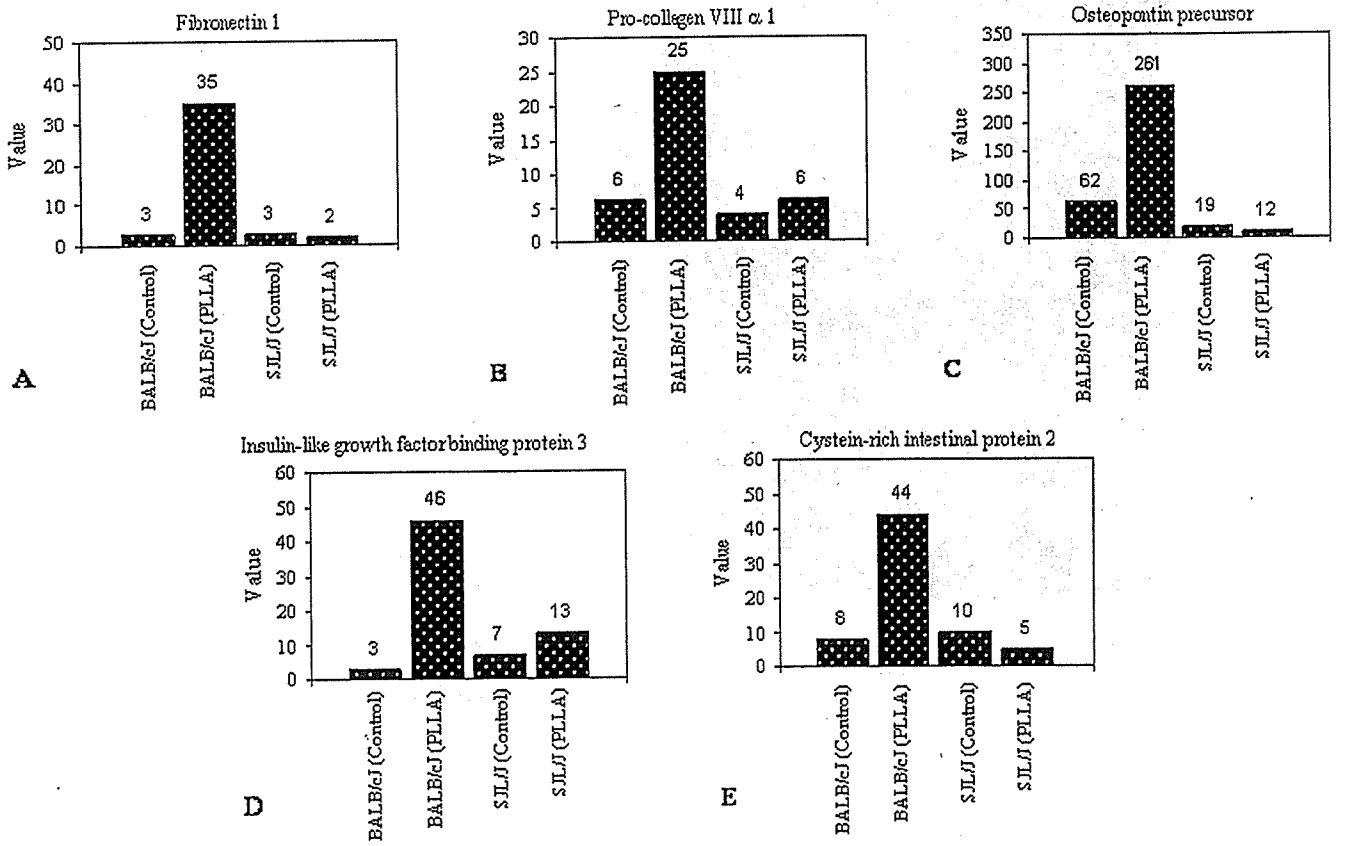

Figure 5. DNA microarray analysis of these four kinds of cells. The expression of (A) fibronectin 1, (B) pro-collagen VIIIα 1, (C) osteopontin precursor (OPN), (D) insulin-like growth factor binding protein (IGFBP) 3, and (E) cysteine-rich intestinal protein 2 (CRIP 2) increased in the cells of PLLA-implanted BALB/cJ mice. Results shown are representative of four independent experiments.

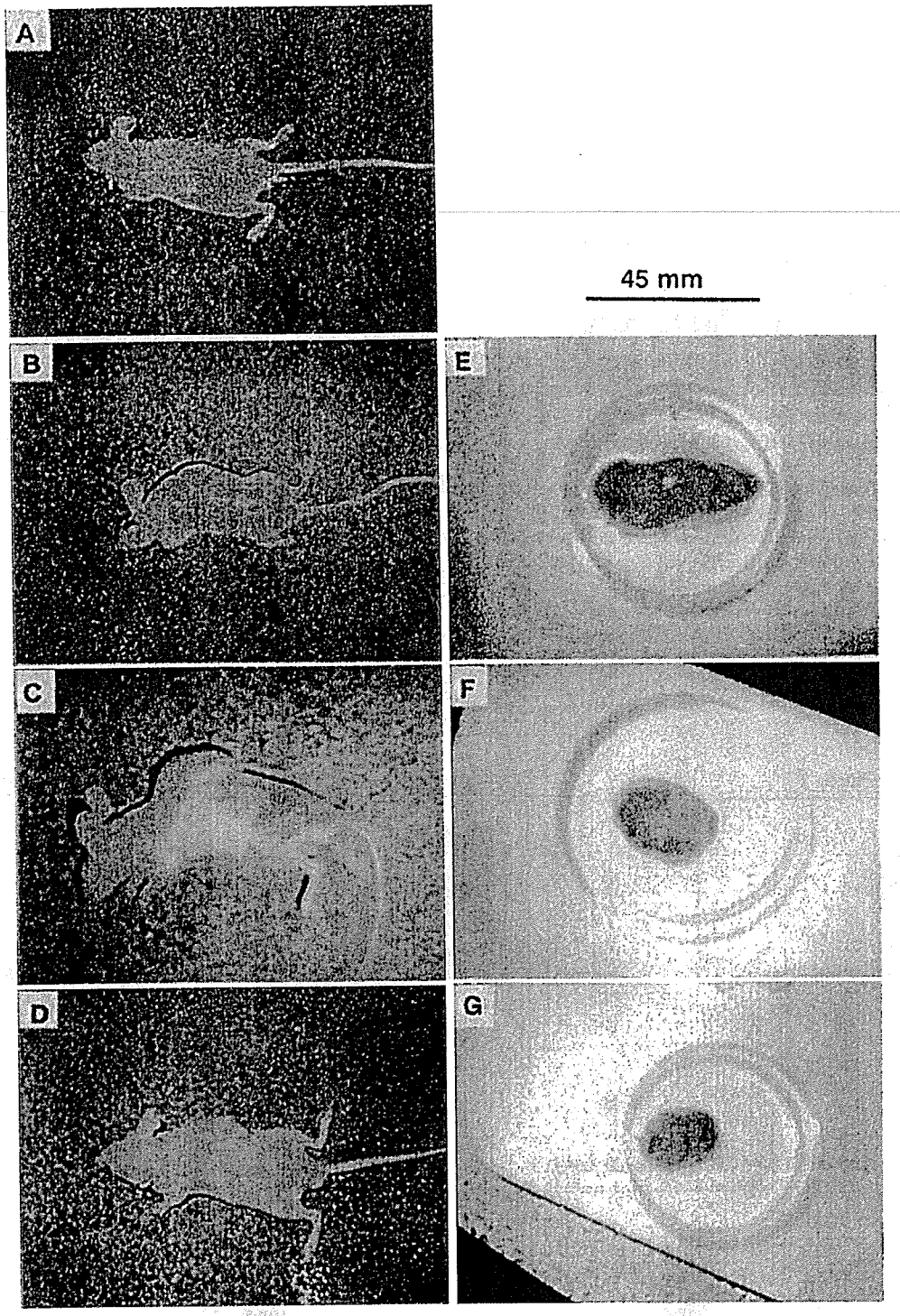

Figure 6. Determination of tumorigenicity in nude mice. (A) No tumor was formed in PBS(−) injected nude mice. (B, C, E, and F) A large tumor growth was observed within two weeks in nude mice injected with cells from PLLA-implanted BALB/cJ mice. (D and G) Tumor growth was observed in nude mice 4 weeks after they were injected with HeLa cells. [Color figure can be viewed in the online issue, which is available at www.interscience.wiley.com.]

and PLLA-implanted groups in SJL/J mice (Fig. 2). We also examined the functional effects on GJIC. In the present study and correlating with our previous report,[22] GJIC was significantly inhibited in PLLA-implanted BALB/cJ mice when compared with that in controls (Fig. 3). Gap junctions are regulated by the post-translational phosphorylation of the carboxy-terminal tail region on the Cx molecule, and hyperphosphorylation of Cx molecules is closely related to the inhibition of GJIC.[28,29] Asamoto et al. reported that tumorigenicity enhanced when the expression of Cx 43 protein was suppressed by the anti-sense RNA of

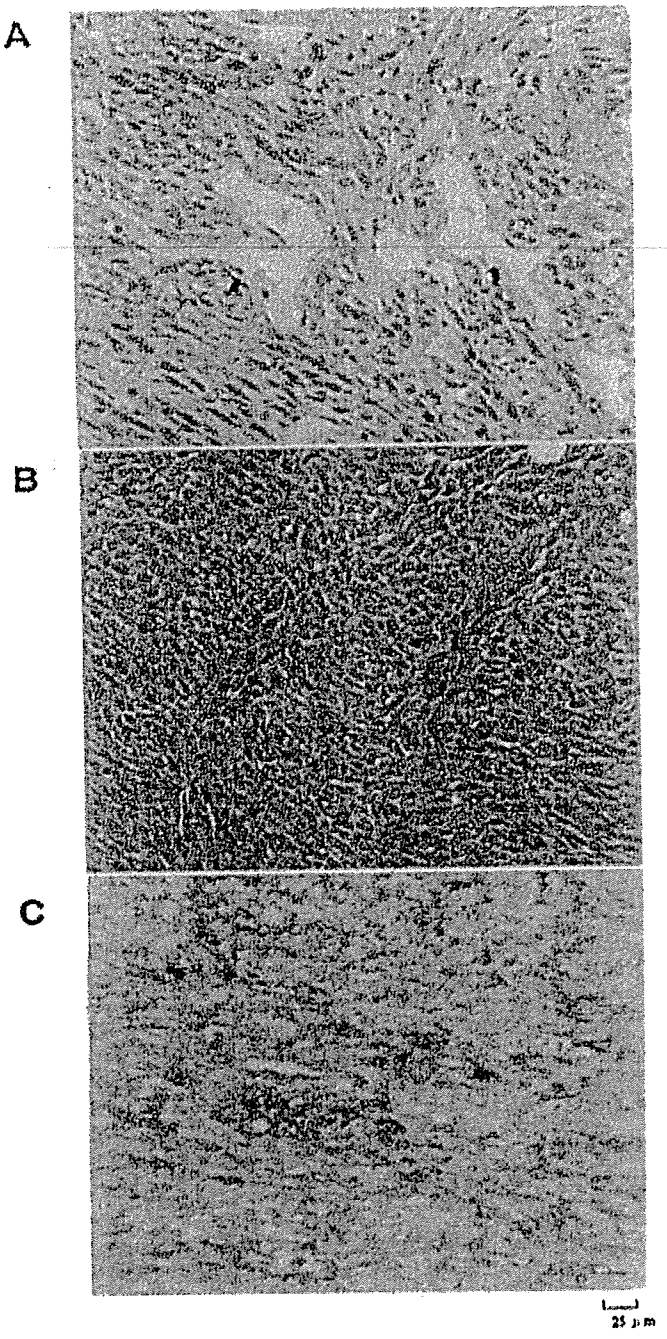

Figure 7. Histopathology. Tumor cells from nude mice injected with cells from PLLA-implanted BALB/cJ mice showed monophasic fibrous synovial sarcoma with H&E and keratin AE1/AE3 staining. (A) Staghorn pattern (H&E), (B) herringbone pattern (H&E), and (C) herringbone pattern (keratin AE1/AE3 staining). [Color figure can be viewed in the online issue, which is available at www.interscience.wiley.com.]

Cx 43.[30] Thus, in our experiment, the impaired GJIC was possibly caused by the suppression of protein expression of Cx 43. Therefore, it is suggested that gap junctions are likely to play a major role in the PLLA-induced tumorigenesis in BALB/cJ mice. But in SJL/J mice, this is not the key factor for tumorigenesis. Another protein may be responsible because Cx 43 protein expression was decreased in both control and PLLA-implanted group of SJL/J mice.

TGF-β1 can impair GJIC function by decreasing the phosphorylated form of Cx 43[31] and can also increase the expression of ECM.[32,33] We estimated the production of TGF-β1 in four kinds of cells. The secretion of TGF-β1 significantly increased in PLLA-implanted BALB/cJ mice cells in comparison with that from BALB/cJ control mice, but TGF-β1 secretion decreased in the SJL/J-implanted group when compared with that in the SJL/J control mice (Fig. 4). Furthermore, by using DNA microarray analysis of these four kinds of cells, expression of the major ECM proteins (fibronectin 1, pro-collagen VIIIα 1, and OPN) and IGFBP 3 was found to be increased in the PLLA-implanted BALB/cJ mice cells (Fig. 5). Several reports have suggested that these proteins could directly cause tumorigenesis.[34–36] Overexpression of CRIP 2, a member of the LIM (characterized by a repeat of a double zinc finger cysteine-rich sequence, CCHC and CCCC) protein family, caused an increase in Th2 cytokine IL-6,[37] and synovial sarcoma cells are reported to produce IL-6 by themselves.[38] Figure 5 shows that IGFBP 3 was highly expressed in the PLLA-implanted BALB/cJ mice cells. In addition, overexpression of IGFBP 3 was associated with poorer prognosis in breast cancer.[36] Therefore, we speculated that overexpression of IGFBP 3 and major ECM proteins directly or indirectly causes tumorigenesis in the PLLA-implanted BALB/cJ mice.

Ten months after implantation of the PLLA plate into BALB/cJ mice, formation of a tissue growth was observed at the implanted site. To determine whether this tissue growth was a tumor or a result of foreign body (PLLA) inflammation, we performed a tumorigenicity assay in nude mice. Rapid growth of a large tumor was observed in nude mice injected with cells obtained from PLLA-implanted BALB/cJ mice (Fig. 6). The histopathologic examination of this tumor disclosed monophasic fibrous synovial sarcoma (Fig. 7). Nude mice injected with HeLa cells as a positive control showed slower tumor growth. However, these PLLA-derived tumor cells did not form a colony in a soft agar assay (data not shown).

We speculated that a protein or regulatory factor other than Cx 43 may play key role in tumorigenesis in PLLA-implanted BALB/cJ mice. In this light, we conclude that overexpression of the regulatory factors such as TGF-β1 and IGFBP 3 caused tumorigenesis in PLLA-implanted BALB/cJ mice. In addition, increased secretion of TGF-β1 suppressed the expression of Cx 43 and inhibited GJIC. Moreover, PLLA increased the expression of ECM, CRIP 2, and OPN. Finally, all these factors in combination promoted tumorigenesis (Fig. 8).

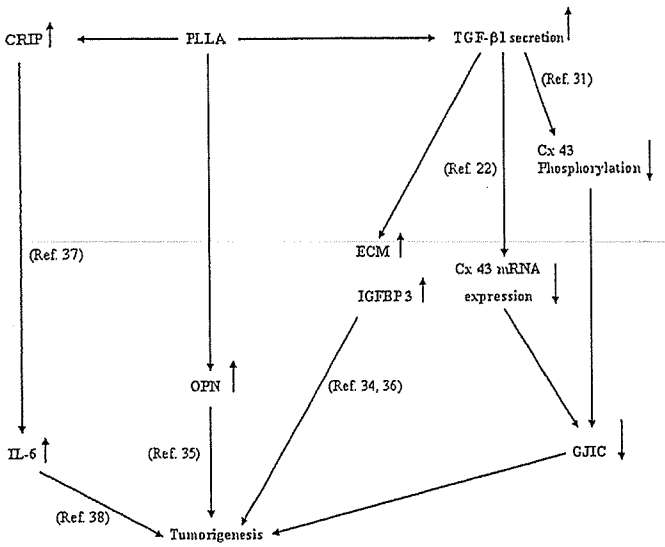

Figure 8. Schematic representation of the pathway of tumorigenesis induced by PLLA in BALB/cJ mice.

References

1. Hayashi T. Interactions between polymers and biosystems: Structure–property relationships in biomaterial polymers. In: Thuruta T, Hayashi T, Kataoka K, Ishihara K, Kimura Y, editors. Biomaterial Applications of Polymeric Materials. Boca Raton, FL: CRC; 1993. pp 17–51.
2. Chesmel KD, Black J. Cellular responses to chemical and morphologic aspects of biomaterial surfaces. I. A novel in vitro model system. J Biomed Mater Res 1995;29:1089–1099.
3. Tang L, Eaton JW. Inflammatory responses to biomaterials. Am J Clin Pathol 1995;103:466–471.
4. Imai Y. Interaction between polymers and biosystem: Biological response to biomedical polymers. In: Thuruta T, Hayashi T, Kataoka K, Ishihara K, Kimura Y, editors. Biomaterial Applications of Polymeric Materials. Boca Raton, FL: CRC; 1993. pp 53–87.
5. Rosengren A, Danielson N, Bjursten LM. Inflammatory reaction dependence on implant localization in rat soft tissue models. Biomaterials 1997;18:979–987.
6. Butler K, Benghuzzi H, Tucci M, Cason Z. A comparison of fibrous tissue formation surrounding intraperitoneal and subcutaneous implantation of ALCAP, HA, and TCP ceramic devices. Biomed Sci Instrum 1997;34:18–23.
7. Kulkarni RK, Pani KC, Neuman C, Leonard F. Polylactic acid for surgical implants. Arch Surg 1966;93:839–843.
8. Craig PH, Williams JA, Davis KW, Magoun AD, Levy AJ, Bogdansky S, Jones JP Jr. A biological comparison of polyglactin 910 and polyglycolic acid synthetic absorbable sutures. Surg Gynecol Obstet 1995;141:1–10.
9. Nakamura T, Shimizu Y, Okumura N, Matsui T, Hyon SH, Shimamoto T. Tumorigenicity of poly-L-lactide (PLLA) plates compared with medical-grade polyethylene. J Biomed Mater Res 1994;28:17–25.
10. Nakamura A, Kawasaki Y, Takada K, Aida Y, Kurokama Y, Kojima S, Shintani H, Matsui M, Nohmi T, Matsuoka A, Sofuni T, Kurihara M, Miyata N, Uchima T, Fujimaki M. Difference in tumor incidence and other tissue responses to polyetherurethanes and polydimethylsiloxane in long-term subcutaneous implantation into rats. J Biomed Mater Res 1992;26:631–650.
11. Trosko JE, Madhukar BV, Chang CC. Endogenous and exogenous modulation of gap junctional intercellular communication: Toxicological and pharmacological implications. Life Sci 1993;53:1–19.
12. Trosko JE, Ruch RJ. Cell–cell communication in carcinogenesis. Front Biosci 1998;3:D208–D236.
13. Falk MM. Biosynthesis and structural composition of gap junction intercellular membrane channels. Eur J Cell Biol 2000;79: 564–574.
14. Evans WH, Martin PE. Gap junctions: Structure and function. Mol Membr Biol 2002;19:121–136. Review.
15. Bruzzone R, White TW, Paul DL. Connections with connexins: The molecular basis of direct intercellular signaling. Eur J Biochem 1996;238:1–27.
16. Loewenstein WR. Junctional intercellular communication and the control of growth. Biochim Biophys Acta 1979;560:1–65.
17. Guthrie SC, Gilula NB. Gap junctional communication and development. Trends Neurosci 1989;12:12–16.
18. Klaunig JE, Ruch RJ. Role of inhibition of intercellular communication in carcinogenesis. Lab Invest 1990;62:135–146.
19. Mesnil M, Yamasaki H. Cell–cell communication and growth control of normal and cancer cells: Evidence and hypothesis. Mol Carcinog 1993;7:14–17.
20. Musil LS, Goodenough DA. Biochemical analysis of connexin43 intracellular transport, phosphorylation, and assembly into gap junctional plaques. J Cell Biol 1991;115:1357–1374.
21. Musil LS, Goodenough DA. Multisubunit assembly of an integral plasma membrane channel protein, gap junction connexin43, occurs after exit from the ER. Cell 1993;74:1065–1077.
22. Ahmed S, Tsuchiya T. A novel mechanism of tumorigenesis: Increased TGF-β1 suppresses the expression of connexin43 in BALB/cJ mice after implantation of PLLA. J Biomed Mater Res A 2004;70:335–340.
23. Brand I, Buoen LC, Brand KG. Foreign-body tumors of mice: Strain and sex differences in latency and incidence. J Natl Cancer Inst 1977;58:1443–1447.
24. El-Fouly MH, Trosko JE, Chang CC. Scrape-loading and dye transfer. A rapid and simple technique to study gap junctional intercellular communication. Exp Cell Res 1987;168:422–430.
25. Tsuchiya T, Hata H, Nakamura A. Studies on the tumor-promoting activity of biomaterials: Inhibition of metabolic cooperation by polyetherurethane and silicone. J Biomed Mater Res 1995;29:113–119.
26. Tsuchiya T. A useful marker for evaluating tissue-engineered products: Gap-junctional communication for assessment of the tumor-promoting action and disruption of cell differentiation in tissue-engineered products. J Biomater Sci Polym Ed 2000; 11:947–959.
27. Nakaoka R, Tsuchiya T, Kato K, Ikada Y, Nakamura A. Studies on tumor-promoting activity of polyethylene: Inhibitory activity of metabolic cooperation on polyethylene surfaces is markedly decreased by surface modification with collagen but not with RGDS peptide. J Biomed Mater Res 1997;35:391–397.
28. Musil LS, Cunningham BA, Edelman GM, Goodenough DA. Differential phosphorylation of the gap junction protein connexin43 in junctional communication-competent and -deficient cell lines. J Cell Biol 1990;111:2077–2088.
29. Lampe PD, Lau AF. Regulation of gap junctions by phosphorylation of connexins. Arch Biochem Biophys 2000;384: 205–215.
30. Asamoto M, Toriyama-Baba T, Krutovskikh V, Cohen SM, Tsuda H. Enhanced tumorigenicity of rat bladder squamous cell carcinoma cells after abrogation of gap junctional intercellular communication. Jpn J Cancer Res 1998;89:481–486.
31. Wyatt LE, Chung CY, Carlsen B, Iida-Klein A, Rudkin GH, Ishida K, Yamaguchi DT, Miller TA. Bone morphogenetic protein-2 (BMP-2) and transforming growth factor-β1 (TGF-β1) alter connexin 43 phosphorylation in MC3T3-E1 Cells. BMC Cell Biol 2001;2:14.

32. Singh LP, Green K, Alexander M, Bassly S, Crook ED. Hexosamines and TGF-β1 use similar signaling pathways to mediate matrix protein synthesis in mesangial cells. Am J Physiol Renal Physiol 2004;286:F409–F416.
33. Kenyon NJ, Ward RW, McGrew G, Last JA. TGF-β1 causes airway fibrosis and increased collagen I and III mRNA in mice. Thorax 2003;58:772–777.
34. Kuchenbauer F, Hopfner U, Stalla J, Arzt E, Stalla GK, Paez-Pereda M. Extracellular matrix components regulate ACTH production and proliferation in corticotroph tumor cells. Mol Cell Endocrinol 2001;175:141–148.
35. Liu SJ, Hu GF, Liu YJ, Liu SG, Gao H, Zhang CS, Wei YY, Xue Y, Lao WD. Effect of human osteopontin on proliferation, transmigration and expression of MMP-2 and MMP-9 in osteosarcoma cells. Chin Med J (Engl) 2004;117:235–240.
36. Rocha RL, Hilsenbeck SG, Jackson JG, VanDenBerg CL, Weng C, Lee AV, Yee D. Insulin-like growth factor binding protein-3 and insulin receptor substrate-1 in breast cancer: Correlation with clinical parameters and disease-free survival. Clin Cancer Res 1997;3:103–109.
37. Cousins RJ, Lanningham-Foster L. Regulation of cysteine-rich intestinal protein, a zinc finger protein, by mediators of the immune response. J Infect Dis 2000;182:S81–S84.
38. Duan Z, Lamendola DE, Penson RT, Kronish KM, Seiden MV. Overexpression of IL-6 but not IL-8 increases paclitaxel resistance of U-2OS human osteosarcoma cells. Cytokine 2002;17:234–242.

Key Engineering Materials Vols. 309-311 (2006) pp. 263-266
online at http://www.scientific.net

Cytotoxicity of Various Calcium Phosphate Ceramics

Masato Tamai[1a], Ryusuke Nakaoka[1b] and Toshie Tsuchiya[1c]
Division of Medical Devices, National Institute of Health Science
1-18-1 Kamiyoga, Setagaya-ku, Tokyo 158-8501 Japan
[a]m-tamai@nihs.go.jp, [b]nakaoka@nihs.go.jp, [c]tsuchiya@nihs.go.jp

Keywords: Calcium phosphate ceramics, Cytotoxicity,

Abstract. The cytotoxicity of five calcium phosphate ceramics, hydroxyapatite (HAp), flouroapatite (FAp), α-tricalcium phosphate (α-TCP), β-tricalcium phosphate (β-TCP) and tetracalcium phosphate (TTCP), was investigated. Based on the guidelines of biological test for medical devices in Japan, a cytotoxicity test of these calcium phosphates was carried out using Chinese hamster V79 lung fibroblasts. The cytotoxic study revealed that FAp and α-TCP showed high cytotoxicities. From various analyses, it was considered that the cytotoxicity of the FAp was due to fluorine ions extracted in a culture medium and the cytotoxicity of α-TCP resulted from a decrease in pH of the medium by the phosphoric acid, which produced by hydrolysis of the α-TCP.

Introduction

From the view point of biological affinity to bone, calcium phosphate (CP) ceramics have been studied to utilize for many purposes in a medical field. For instance, hydroxyapatite ($Ca_{10}(PO_4)_6(OH)_2$, HAp) and β-tricalcium phosphate (β-$Ca_3(PO_4)_2$, β-TCP), are known to be biologically bonded to natural bones and their porous materials have been studied for effective restoration of bone defects.[1,2] Fluoroapatite ($Ca_{10}(PO_4)_6F_2$, FAp) has been reported to have a potential of novel bone repairing materials with high stability *in vivo*, since solubility of FAp is lower than that of HAp.[3,4] In addition, CP cement is also promising for bone repair and it is well known that α-tricalcium phosphate (α-$Ca_3(PO_4)_2$, α-TCP) and tetracalcium phosphate ($Ca_4(PO_4)_2O$, TTCP) are starting materials for the harden reaction of the bone cement.[5,6]

To develop biomaterials for utilizing for bone tissue, various properties, e.g. biological, physical and chemical property, should be satisfied. Among them, biological safety is important for the biomaterials. Since only a few studies which discuss the cytotoxicity of calcium phosphate ceramics have been reported, the cytotoxicity of CP ceramics is worthy to be investigated in order to design bioceramics with good biological safety for medical application. Therefore, the cytotoxicities of five calcium phosphate ceramics, hydroxyapatite (HAp), flouroapatite (FAp), α-tricalcium phosphate (α-TCP), β-tricalcium phosphate (β-TCP) and tetracalcium phosphate (TTCP) were investigated.

Materials and Methods

Materials

Five kinds of CP ceramics, HAp, FAp, α-TCP, β-TCP and TTCP were purchased from Wako chem. Co. Ltd. CP powders (0.25 g) was put into stainless mold and uniaxially pressed at 30MPa for 1 min to form a pellet. The dimensions of the obtained CP pellet were 1mm in thickness and 12mm in diameter. CP pellets were sterilized by an autoclave at 121°C for 20 min.

Cytotoxicty test on CP ceramics

Cytotoxicity test was carried out using Chinese hamster V79 lung fibroblasts by a colony assay system. V79 cells were maintained in Eagle's minimum essential medium (Nissui Pharmaceutical Co. Ltd.) with 10% fetal calf serum (FCS, Intergen Co. Ltd.) and incubated at 37 °C in a humidified atmosphere with 5% CO_2.

The method of cell seeding in the cytotoxicity test of CP ceramics was shown below; each CP pellets were placed in each culture wells of 24 well culture plates (Corning Co. Ltd.) and 300μl of culture medium was added into each well. Then, 50 cells/300μl of the cell suspension in the

culture medium were added into each well and incubated at 37°C for 4 h. Finally, 400μl of the culture medium was added into each well and the plates were incubated at 37 °C in a humidified atmosphere with 5 % CO_2 for 7days. In order to investigate a cell adhesive property on the CP ceramics, the culture medium was changed after 4 h and further incubated for 7days. The removed culture medium was transferred to another well of a new plate and incubated for 7days as well.

Cytotoxicity of extracts from CP ceramics was also investigated in this study. Suspensions of CP ceramics in the culture medium (100mg/mL) were stirred at 37°C for 3days under the rotation condition at 150rpm. The suspensions were centrifuged and the supernatants were collected as test extracts. In addition, media with various pH values were prepared using HCl solution to investigate an effect of pH on cell survival. Fifty V79 cells in 1ml of the extracts or the medium with different pH value were incubated at 37 °C for 7days.

After 7-day incubation, the cells were fixed in methanol and the number of the V79 colonies was counted after staining cells with 5%-Giemsa solution to estimate the cytotoxicity of the test sample. In addition, the pH of the medium after 7-days culture was measured to estimate the effect of the pH of the medium on the cytotoxicity test.

Characterization of CP ceramics

The structural changes of CP before and after an autoclave-sterilization or an incubation at 37°C culture were investigated by powder X-ray diffraction (XRD) analysis and scanning electron microscopy (SEM). XRD analysis was carried out (Rigaku Co., Ltd. / RINT 2000) with the CuK_α radiation at 40kV, 50mA. SEM observations were performed (JEOL / JSM-5800LV) with an accelerating voltage of 25kV.

Results and Discussion

Cytotoxicity of various CP ceramics

From XRD analysis, no structural changes of CPs were observed after an autoclave sterilization. After staining CP pellets, it was observed that cell colonies were formed on various CP ceramics pellets (Fig.1(a)). The results of the cytotoxicity test of CPs are shown in Fig.1(b). The cell colonies were hardly formed on FAp and α-TCP pellets and the ratios of the colonies formed on these pellets against V79-alone culture were 22.6% and 0.0%, respectively. In addition, the ratios of the colonies on the HAp, β-TCP and TTCP pellets were 58.1%, 57.3% and 78.4%, respectively. As no colonies were observed after 7-day culture of the removed medium in cell adhesion studies of CP ceramics, these results suggested that V79 cells can adhere and be viable on these pellets, irrespective of the type of CP ceramics. Figure 2 shows the formation of colonies cultured in extract from CP ceramics. The cytotoxicity test of extracts from CPs revealed that the tendency of their cytotoxicities was similar to that of the cytotoxicities on the respective CP pellets themselves (Fig.1(b)).

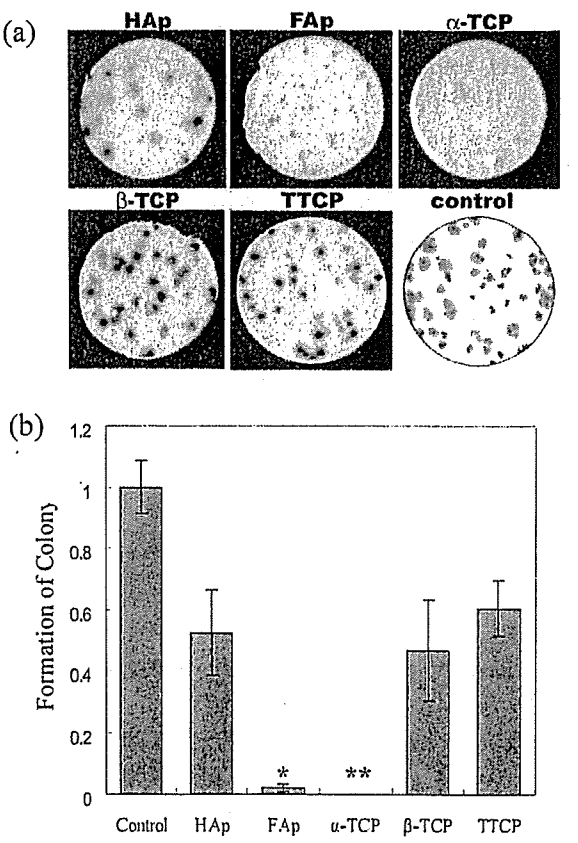

Fig.1. The appearance of colonies on various CP pellets (a) and their colony formation ratios (b). (*$p<0.05$ against for V79 alone, **$p<0.01$ against for V79 alone)

The fact that less formation of colonies was observed on FAp and α-TCP pellets suggests that they are highly cytotoxic. In addition to results shown in Fig.2, it is suggested that the differences in the colony formation ratio on various CP pellets are ascribed to difference in extract properties from the CP, which may be related with the composition or crystal structure. As shown in Table 1, the pH of culture medium after incubation with FAp pellets is almost the same as that of HAp, while the pH of the α-TCP-incubated medium is much lower than that of the other CP ceramics-incubated media.
In order to consider the reason of the low pH of the a-TCP-incubated medium, a surface structural change of α-TCP before and after incubation was analyzed by SEM. SEM images of α-TCP before and after extraction treatment are shown in Fig.3. Before extraction, a particle size of α-TCP was about 10μm and its surface was smooth (Fig.3(a) and (b)). However, whisker-like precipitates of 1-2μm in length and 2-300nm in width were observed at the surface of α-TCP after the extraction, although there was no change in its particle size (Fig.3(c) and (d)). It is well known

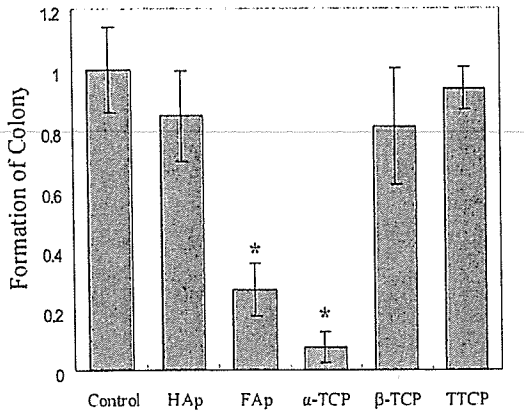

Fig.2. Formation of colony cultured in extract from various CP ceramics. (*p<0.01 against for V79 alone)

Table 1. The pH and Ca concentration of culture medium after incubation.

Samples	pH of medium after culturing	Ca concentration /ppm
V79 alone	7.12	-
HAp	7.24	0.19
FAp	7.20	0.17
α-TCP	6.76	72.62
β-TCP	7.40	1.27
TTCP	7.65	0.58

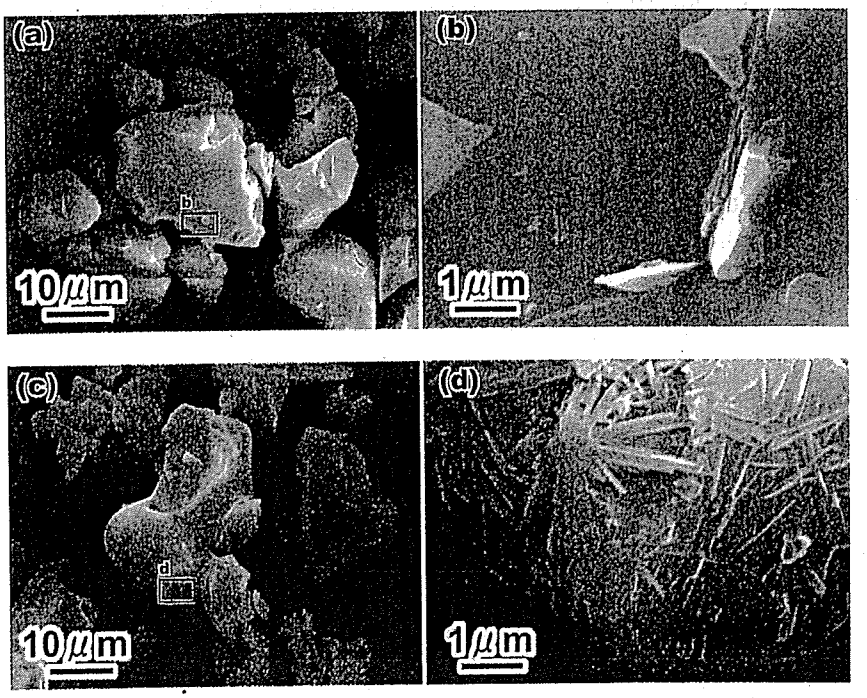

Fig.3. SEM images of α-TCP before (a), (b) and after extract treatment (c), (d). (a) and (c) are whole image of before and after extract treatment, respectively. (b) and (d) are enlarged image of the area enclosed by a rectangle in (a) and (c), respectively.

that calcium phosphates convert to HAp in aqueous solution with high pH value. Since the solubility of α-TCP is higher than that of other calcium phosphates, α-TCP rapidly converts to HAp as follows;

$$10Ca_3(PO_4)_2+6H_2O \rightarrow 3Ca_{10}(PO_4)_6(OH)_2+2H_3PO_4$$

According to the report of this conversion [7], HAp produced by the above reaction has whisker-like morphology. Therefore, the whisker-like precipitates in Fig.3 (d) can be regarded as HAp, so that it is considered that the above conversion occurs at the surface of the α-TCP during incubation.

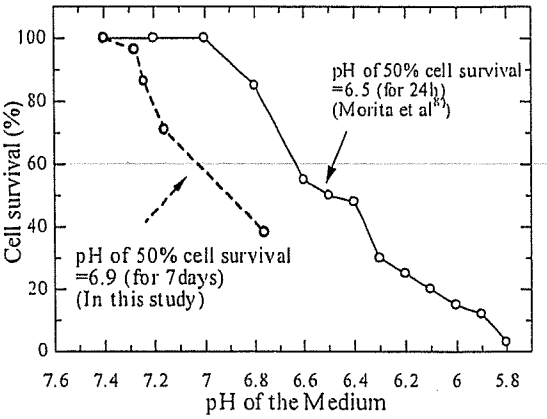

Fig.4. V79 cell survival in the medium with various pH values.

In this case, phosphoric acid is produced as a byproduct in the conversion reaction and the phosphoric acid causes the decrease in pH of the solution. As shown in Fig.4, Morita and co-workers[8] have reported that low pH itself could be clastogenic to mammalian cells and the pH of 50% V79 cell survival was 6.5 for 24h incubation. In the present colony assay system, the pH of 50% V79 cell survival was 6.9 for 7-days incubation. In addition, we confirmed that phosphoric acid showed no or weak cytotoxicities under our present experimental conditions. Therefore, it is suggested that the cytotoxicity of α-TCP is mainly due to the pH decrease resulting from an increase of the phosphoric acid ion by the hydrolysis conversion from α-TCP to HAp.

On the other hand, FAp has the same crystal structure of HAp but the hydroxyl ions in HAp substituted by fluorine ions. Since it is probable that difference of the colony formation on various CP ceramics are due to eluted substances from CP as described above, the cytotoxicity of FAp would be due to eluted fluoride ions from FAp. In conclusion, this study has revealed that FAp and α-TCP have a cytotoxicity, while TTCP has lower cytotoxicity than other calcium phosphates. To develop biomaterials made from calcium phosphate, further studies are necessary to clarify their cytotoxic mechanisms.

Acknowledgment

This study was supported in part by a Grant-in-Aid for Scientific Research on Advanced Medical Technology from Ministry of Labour, Health and Welfare, Japan and a Grant-in-Aid from Japan Human Sciences Foundations.

References

[1]Y.Ito, N.Tanaka, Y.Fujimoto, Y.Yasunaga, O.Ishida, M.Agung and M.Ochi: J. Biomed. Mater. Res. Vol.69A (2004), p.454
[2]Y.Wang, T.Uemiura, J.Dong, J.Tanaka and T.Tateishi: Tissue Eng. Vol.9 (2003), p.1205
[3]S.M.Barinov, F.Rustichelli, P.V.Orlovskii, A.Lodini, S.Oscarsson, A.S.Firstov, V.S.Tumanov, P.Millet and A.Rosengren: J.Mater.Sci:Mater in Med. Vol.15 (2004), p.291
[4]K.Cheng, W.Weng, H.Qu, P.Du, G.Shen, G.Han, J.Yang and M.J.Ferreira: J. Biomed. Mater. Res. B Vol 69 (2004), p.33
[5]E.L.Carey, H.H.Xu, G.C.Simon, S.Takagi and C.L.Chow: Biomaterials Vol 26 (2005), P.5002
[6]M.E.Ooms, J.G.C.Wolke, J.P.C.M.Waerden and J.A.Jansen: J. Biomed. Mater. Res.Vol.61 (2002), p.9
[7]M.Tamai, T.Isshiki, K.Nishio, M.Nakamura, A.Nakahira and H.Endoh: J. Mater. Res. Vol.18 (2003), p.2633
[8]T.Morita, T.Nagaki, I.Fukuda and K.Okumura: Muta. Res. Vol.268 (1992), p.297

Available online at www.sciencedirect.com
SCIENCE DIRECT®
Biomaterials 27 (2006) 1437–1443
Biomaterials
www.elsevier.com/locate/biomaterials

The effect of hyaluronic acid on insulin secretion in HIT-T15 cells through the enhancement of gap-junctional intercellular communications

Yuping Li[a,1], Tsutomu Nagira[a,b], Toshie Tsuchiya[a,*]

[a]*Division of Medical Devices, National Institute of Health Sciences, 1-18-1 Kamiyoga, Setagaya-ku, Tokyo 158-8501, Japan*
[b]*Japan Association for the Advancement of Medical Equipment, 3-42-6 Hongo, Bunkyo-ku, Tokyo 113-0033, Japan*

Received 28 April 2005; accepted 11 August 2005
Available online 19 September 2005

channel and connexin-43 (Cx43) expression by its actions on focal adhesions and the associated cytoskeleton [5]. In addition, Park and Tsuchiya [6] have reported that high molecular weight (HMW) HA-coating can enhance the function of gap-junctional intercellular communications (GJIC). The insulin secretion from pancreatic β-cells is a multicellular event depending on their interaction with neurotransmitters and numerous signal molecules carried by blood and also direct interactions between cell–cell and cell–matrix contacts by gap-junctional channels, which mediate exchanges of molecules smaller than 1000 Da, such as ions, small metabolites, and second messengers between adjacent cells. The latter interactions are thought to be crucial regulatory mechanisms of insulin secretion [7–9], and the pharmacological blockade of GJIC markedly decreases insulin release [8]. However, the effects of HMW HA as biomaterials of support matrix on functions of pancreatic β-cells and gap-junctional channel remain unclear.

In the present study, we investigated the effects of HMW HA on the function of GJIC, the expression of Cx43, insulin content, and insulin secretion using HIT-T15 cells in vitro. These results suggest that HMW HA can be used as the biomaterial for the development of a bioartificial pancreas: design biocompatibility of HA depends on the molecular-weight size of HA, and its application method and concentration.

2. Materials and methods

2.1. Materials

Lucifer yellow was purchased from Molecular Probes (Eugene, OR). HA (1680 kDa) and TetraColor ONE (WST-8) were supplied by Seikagaku Industries, Ltd. (Tokyo, Japan). ELISA insulin assay kit was obtained from Morinaga Seikagaku Co. (Yokohama, Japan). Bovine serum albumin (BSA) was obtained from Roche Diagnostics GmbH (Mannheim, Germany). Krebs–Ringer bicarbonate (KRB) buffer (pH 7.4), fetal bovine serum (FBS), and anti-Cx43 were purchased from Sigma Chemical Co. (St. Louis, MO). β-actin antibody was obtained from Cell Signaling Technology Inc. (Tokyo, Japan). Roswell Park Memorial Institute (RPMI) 1640 medium was from Nissui pharmaceutical Co. (Tokyo, Japan). All other chemicals used were obtained from Wako Pure Chemical Industries (Osaka, Japan).

2.2. Preparation of media and culture dishes

The HA polysaccharide was dissolved in distilled water at a concentration of 4 mg/ml. Each of the 35-mm culture dish (Falcon 1008, Becton Dickinson) was coated at a final concentration of 0.01, 0.05, 0.1, 0.5, and 1.0 mg/ml. The HA-coated dishes were dried further under sterile air flow at room temperature for 12 h before use. In order to investigate the effect of HA-addition on the functions of HIT-T15 cells, different media were prepared at a final concentration of 0.01, 0.05, 0.1, 0.5, and 1.0 mg/ml. HA-treatment is performed to cells for 24 h.

2.3. Cells and cell culture

A hamster pancreatic β-cell line, HIT-T15 (HIT-T15 cells, Dainippon Pharmaceutical Co., Japan), was cultured in RPMI 1640 medium containing 10% FBS, 2 mM L-glutamine, 100 IU penicillin-G and 100 μg/ml streptomycin at 37 °C in a humidified atmosphere of 5% CO_2. The subculture cells were seeded at a density of $1.0–5.0 \times 10^5$ cells/ml in multiwell plates or culture dishes. When they reached more than 80% confluence, the cells were used for various studies. Throughout the cell growth period the culture media were replaced every 2 days.

2.4. Measurement of cell viability

To evaluate the affect of HMW HA on cell viability of HIT-T15 cells, HIT-T15 cells (1×10^5) were incubated into the various concentrations of HA-coated 24-well plates, or after the cells were seeded onto 24-well plates and pre-incubated in a 10% FBS/RPMI 1640 medium overnight, the medium was exchanged for 10% FBS/HA/RPMI 1640 medium prepared. After 24 h of HA-treatment, the cell viability was determined by the WST-8 reduction assay, according to the manufacturer's instructions. Control cells received fresh medium without HA.

2.5. Measurement of insulin release and insulin content

HIT-T15 cells were treated as described above. After pre-incubating for 30 min at 37 °C in KRB buffer, no glucose cells were stimulated for 60 min with 11.1 mM glucose in KRB buffer. The medium was collected, centrifuged for 5 min at 3000*g*, and the supernatant was frozen at −80 °C for insulin release assay. Cultures were then extracted for 24 h at 4 °C in acid-ethanol and the extracts also frozen for determination of insulin and protein content. Insulin was determined by ELISA insulin kit with rat insulin as standard, according to the manufacturer's instructions. Protein content was measured by the BCA protein assay reagent kit with albumin as standard (PIERCE). Values of secreted insulin were normalized to protein content.

2.6. Measurement of dye transfer

Gap junction-mediated communication between β-cells regulates the insulin secretion and insulin biosynthesis. Because HMW HA-coating increased the insulin release and insulin content but not HA-added, we tested whether the HA-coating increases the insulin secretion and insulin content have a relationship with gap junctions between HIT-T15 cells. HIT-T15 (5×10^5) cells were exposed to the HA-coated (0.1, 0.25, and 0.5 mg/dish) 35-mm glass coverslip (Ashland, MA) and incubated for 24 h to evaluate dye coupling using Lucifer yellow. The cells were rinsed with phosphate-buffered saline [PBS(+)] containing Ca^{2+}/Mg^{2+}, and 3 ml of PBS(+) containing 1% BSA and 10 mM HEPES (pH 7.4) were added to keep a sufficient pH stability under the microscope. The junctional coupling of HIT-T15 cells was determined by injecting Lucifer yellow into individual cells within monolayer clusters. Injections were performed on a phase-contrast microscope with InjectMan NI2 and microinjector FemtoJet (Eppendorf AG, Germany) using glass micropipette that were filled with a 4% solution of Lucifer yellow CH (MW 457.2) dissolved in 0.33 M lithium chloride, as previously described [11]. An injection pressure of 6.5 psi for 200 ms was used for each injection. The coupling extent was evaluated by counting dye-transferred cells at 2 min after microinjection. There was no leakage of injected dye into the medium.

2.7. Western blot analysis

HIT-T15 cells were grown into the various concentration of HA-coated 100-mm plastic dishes (0.1, 0.25, and 0.5 mg/dish) (FALCON 3003; Falcon) for 24 h, rinsed with Ca^{2+}/Mg^{2+}-free PBS(−) and then lysed in CelLytic™-M lysis/extraction reagent (Sigma). Protein content was measured by the BCA protein assay reagent kit (PIERCE). Samples of total extracts (20 μg protein/lane) were fractionated by eletrophoresis in a 10% sodium dodecyl sulfate polyacrylamide gel electrophoresis (SDS–PAGE). The contents of the gels were transferred to PVDF membranes (Clear Blot Membrane-P). Membranes were saturated for 2 h at room temperature in Block Ace (Dainippon Pharmaceutical Co.,

Japan) and then were incubated with antibodies directed against Cx43 (1:1000) and β-actin (1:1000) as the primary antibody overnight at 4 °C. After repeated rinsing in PBS–Tween, the immunoblots were incubated with a peroxidase-conjugated antibody against rabbit (1:5000) at room temperature for 1 h. Membranes were developed by enhanced chemiluminescence according to the manufacturer's instructions (Amersham Pharmacia Biotech).

3. Results

3.1. Cell viability

In order to evaluate the affect of HMW HA on cell viability, HIT-T15 cells were incubated with HA-coated (0.01, 0.05, 0.1, 0.5, and 1.0 mg/dish) or -added (0.01, 0.05, 0.1, 0.5, and 1.0 mg/ml) for 24 h. After 24 h exposure to HA-added, there was no significant change in the viable HIT-T15 cell number at the low concentration of HA-added ($\leqslant$1.0 mg/dish) compared to control. In contrast, after 24 h of incubation, the cell viability of HIT-T15 cells grown on high concentration HA-coated dishes ($\geqslant$1.0 mg/dish) was significantly less than on low concentration HA-coated and control (Fig. 1). Therefore, all further studies were conducted using low concentration of HA ($\leqslant$0.5 mg/dish).

3.2. Insulin secretion and insulin content

HIT-T15 cells, retain glucose-stimulated insulin secretion, showed an increase in insulin secretion as a function of stimulation. Thus, their insulin output was 2.73±0.36 and 3.90±0.41 pg/μg protein in the base and glucose-stimulation (11.1 mM), respectively (n = 9 dishes from three independent experiments). When these cells were exposed to a low concentration of HA-coating (0.1, 0.25, and 0.5 mg/dish) for 24 h, their insulin secretion was significantly increased in the presence of glucose-stimulation (Fig. 2). However, in contrast, when HIT-T15 cells were incubated with HA-addition for 24 h, the increasing effect was not exhibited. The insulin secretion was without a difference between control and HA-addition (Fig. 2). On the other hand, after acid-ethanol extraction, we found that the insulin content of the HIT-T15 cells grown onto the HA-coated dishes was significantly increased but not HA-added (Fig. 3).

GJIC and Cx43 are thought to be crucial regulatory mechanisms of insulin secretion and insulin content. As described above, HA-coating increased insulin secretion and insulin content of the HIT-T15 cells. In addition, Park and Tsuchiya [6] reported that HMW HA-coating can enhance the function of GJIC in normal human dermal fibroblasts but not HA-addition. Hence, all further studies on the mechanism of insulin secretion and insulin content were conducted using HA-coating.

3.3. Dye transfer

We assessed the function of GJIC using Lucifer yellow by counting the number of dye-transferred cells at 2 min

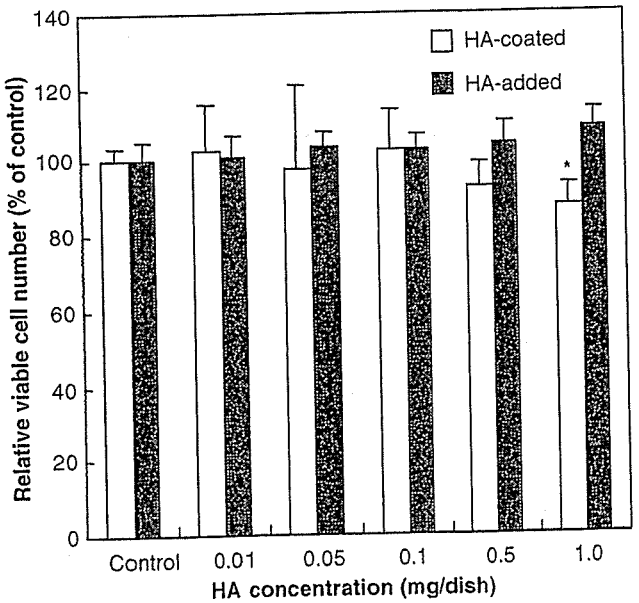

Fig. 1. Concentration-dependent effects of HA-treatment on viability of HIT-T15 cell. After HIT-T15 cells were incubated with HA-coated or HA-added for 24 h, the viable cell numbers of HIT-T15 cell were determined by WST-8 assay as described in methods. Each value denotes the mean±S.D. of three separate experiments. *$P\leqslant0.05$ compared to control under the HA-coated condition.

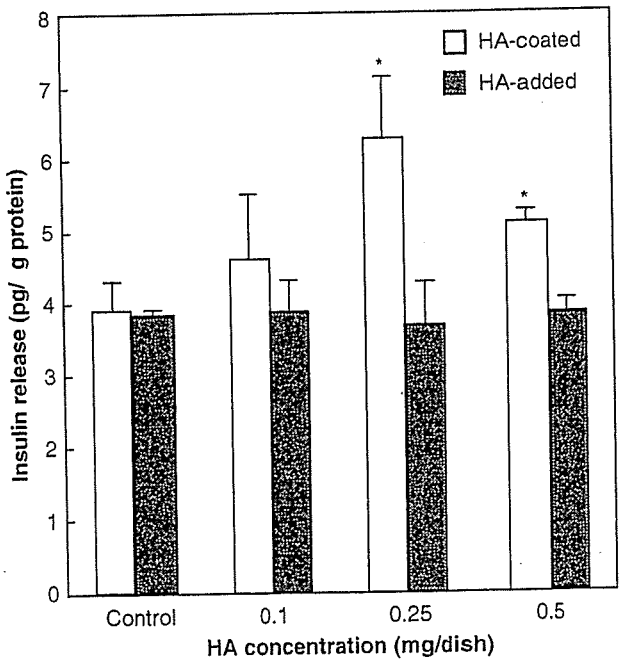

Fig. 2. Insulin secretion from HIT-T15 cells by HA-treatment. HIT-T15 cells were incubated with HA-coating (□) or HA-added (■) for 24 h and then stimulated for 60 min with 11.1 mM glucose in KRB buffer. The released insulin in the spent medium was determined by ELISA insulin kit. Each value denotes the mean±S.D. of three separate experiments. *$P\leqslant0.05$, compared to control in the presence of glucose.

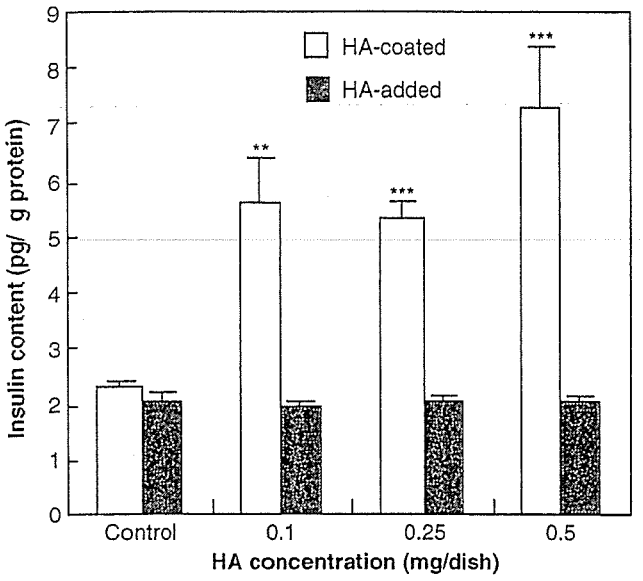

Fig. 3. Insulin content of HIT-T15 cells incubated with HA-coated (□) and HA-added (■). Cells were incubated in the presence of different HA concentrations (0.1–0.5 mg/dish) for 24 h and then stimulated for 60 min with 11.1 mM glucose. The insulin content in the extracts was determined by ELISA insulin kit. Each value denotes the mean ± S.D. of three separate experiments. $^{**}P \leq 0.01$ and $^{***}P \leq 0.001$ compared to control.

after microinjection. Fig. 4A shows the patterns of dye transfer in HIT-T15 cells treated with HA-coating (0.1, 0.25, and 0.5 mg/dish) for 24 h. Most microinjections led to the intercellular transfer of Lucifer yellow, indicating the frequent coupling of HIT-T15 cells. Under control conditions, microinjection experiments revealed that 47.1% of HIT-T15 cells transferred Lucifer yellow with a limited number (1.5 ± 0.6) of microinjection cells. In HA-coated conditions, almost injected cells (95%) showed Lucifer yellow dye transfer, the number of Lucifer yellow-transferred cells (3.2 ± 1.3, 4.4 ± 1.9, and 4.1 ± 1.9, respectively) was more than that of the control condition ($P < 0.001$) (Fig. 4B), which indicated that GJIC function was activated by the HA-coating.

3.4. Cx43 expression

Cx43 is the 43-kDa member of a conserved family of membrane spanning gap-junction proteins. To provide further evidence that the HA-coating increased the function of GJIC, relative to the levels of actin, comparable levels of immunolabeled Cx43 was detected in 0.1, 0.25, and 0.5 mg/dish of HA-coating cells. Whole cell lysates from HA-coated dish were subjected to SDS–PAGE. Immunoblot analysis was performed with an antibody that specifically recognized Cx43 or β-actin. A Western blot analysis revealed that Cx43 proteins are present in cultured HIT-T15 cells in three forms at 43 kDa region, consisting of a nonphosphorylated form and phosphorylated forms (P1 and P2). HA-coating appeared to induce a greater concentration-dependent increase in all three Cx43 protein levels than control. However, the protein level of β-actin was no different from them (Fig. 5), indicating HA-coating increases the function of GJIC via the expression of Cx43. To account for differences in loading, proteins were both stained with Coomassie blue and immunolabeled for β-actin. The latter staining, which did not change in our experiments relative to that of Coomassie blue (data not shown), was used as an internal standard. These results suggested that HA-coating specifically increased the Cx43 protein but not all cell proteins of HIT-T15 cells.

4. Discussion

The transplantation strategy of bioartificial pancreas is to construct bioartificial tissues in vitro from cells or islets and a support matrix and implant the construct into the body in place of the original. The support matrix must be able to maintain the functions of differentiated cells or contain and/or be able to release appropriate biological signaling information to promote and maintain cell adhesion and differentiation. HA is a high-molecular-mass polysaccharide of support matrix in the body, which is believed to play roles in maintaining various physiological functions including water and plasma protein homeostasis, cell proliferation, cell locomotion, and migration [3]. HA is plentiful, easy to extract and mold into a variety of shape, and biodegradable. It is thus widely used matrix biomaterial for bioartificial tissues [10]. In this study, we investigated whether administration of various concentration of HMW HA influences the viability, GJIC, and insulin secretion of pancreatic β-cells as a matrix biomaterial of bioartificial pancreatic constructs.

Previous study has shown that HMW (310 and 800 kDa) HA-coating (2.0 mg/dish) resulted in low adhesiveness to the cells and the decrease of viability in normal human dermal fibroblasts, because of the change in GJIC functions and induction of various genes including cytokines, adhesion molecules, and growth factors [6,11,12]. In the present study, similar results were obtained. After 12 h, the HIT-T15 cells grown into low concentration HA-coated dishes (0.1, 0.25, and 0.5 mg/dish) and control cells already had attached and confluent but not high concentration HA-coated dishes (≥1.0 mg/dish). We showed that treatment with high concentration of HMW (1680 kDa) HA-coated dose dependently inhibited the viability of HIT-T15 cells. In contrast, there was no difference in viability of HIT-T15 cells between the control and HA-added dishes. These results indicated that among the individual qualities of ECM, the viscosity plays a decisive role. The changes of cell viability by HA-treatment may depend on the cell attachment activity. The difference in cell attachment activity may depend on the surface structure of the coated HA, because the HMW HA-coated surface provides a stable anionic surface that prevents cells attachment at the early time [13]. This result suggests that the molecular-weight size of HA and its

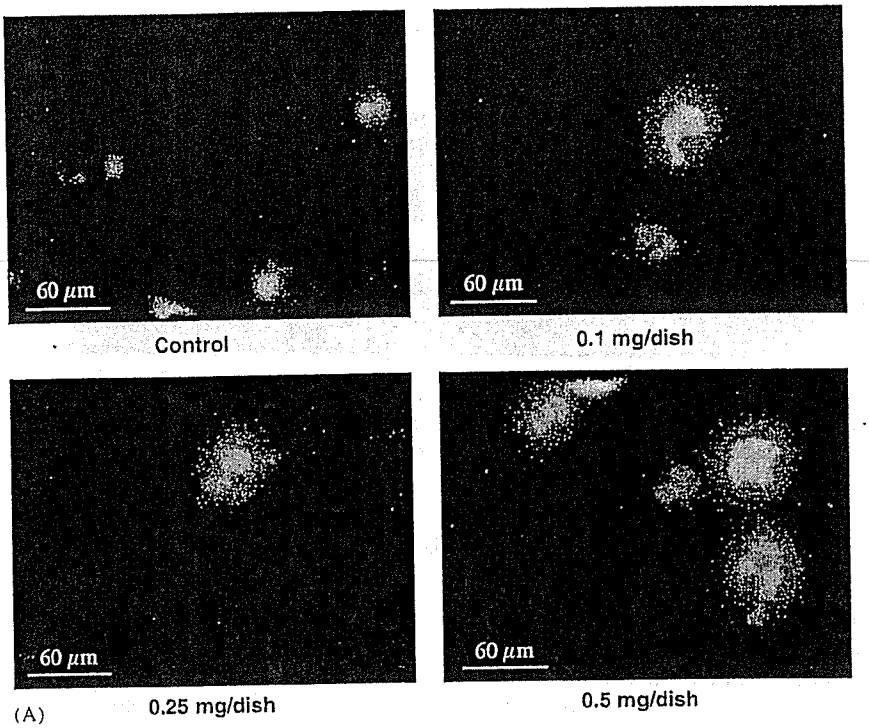

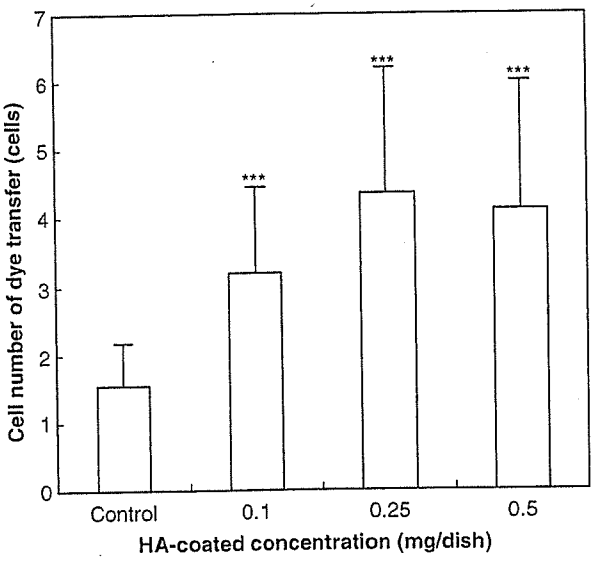

Fig. 4. Concentration-dependent effects of HA-coating on dye transfer in HIT-T15 cells. Cell adherent to glass coverslips were microinjected with 4% Lucifer yellow. Transfer of dye to neighboring cells was assessed by epifluorescence microscopy 2 min later. This is a representative expression of 18 injections per group (A). The number of neighboring cells that received dye was quantified (B). Each value expressed as the mean ± S.D. ($n = 18$). *** $P \leqslant 0.001$ compared to control.

application method and concentration are important factors for generating biocompatible tissue-engineered products.

It has been reported that single β-cells (which cannot form gap junctions) show alterations in both basal and stimulated release of insulin, in protein biosynthesis, and in the expression of the insulin gene. The sustained stimulation of insulin release is associated with an increase in β-cells coupling, in the expression of gap junctions by a unique mechanism for direct equilibration of ionic and molecular gradients between nearby cells [14–16]. In this study, we found that the insulin release and insulin content are increased and GJIC activity was enhanced in cultured HIT-T15 cells by low concentration HMW HA-coating in spite of the inhibitory effects on the cell viability in high concentration HA-coating dishes. This finding was consistent with previous reports. The effect of HA may be influenced by the viscosity of HA, the concentration of

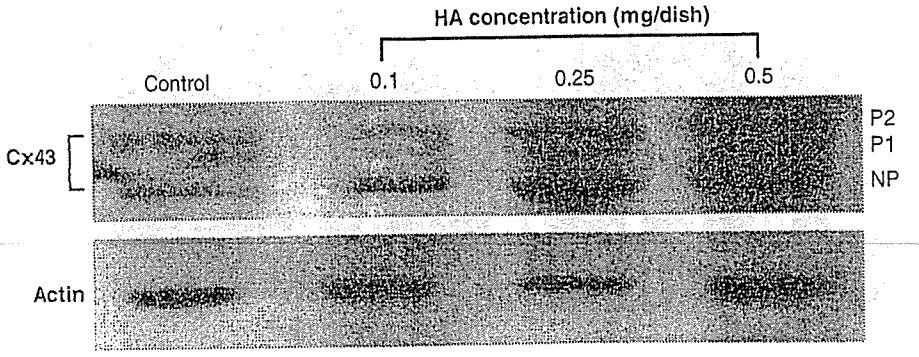

Fig. 5. Identification of Cx43 in HIT-T15 cells grown on the HA-coating dish by Western blot analysis. After HIT-T15 cells were incubated into HA-coated dish for 24 h, cells were lysed and proteins (20 μg) were separated by SDS–PAGE followed by Western blotting using rabbit anti-Cx43 antibody. Actin immunostaining was used to assess equivalent protein loading. This is a representative autoradiogram of three experiments.

FBS and the nutrients in media such as hormone, growth factor (FGF, etc.), cell adhesion molecule (N-CAM and cadherins), and transportation protein [6,17]. As a result, the HIT-T15 cells can use these nutrients and the nutrient-enriched substrata (e.g. natural ECMs) by ionic interaction and the binding of HMW HA to various kinds of cytokines, to change the cell aggregations, resulting in the increase of GJIC. With the evidence above, the enhancement of GJIC activity induced by HA-coating participated in the regulation of insulin release and insulin biosynthesis. On the other hand, the glucose stimulus-secretion coupling in β-cells generated several signals, including a signal to secrete preformed insulin stored in secretory vesicles, a signal, which may be the same or different, to secrete newly made insulin, and a signal to synthesize more insulin. The mechanism of glucose-induced insulin secretion is distinct from that of glucose-induced proinsulin biosynthesis and insulin gene transcription [18]. Moreover, the qualities of ECM affect the insulin release [19]. Therefore, it is possible that HA-coated dishes promoted a large increase in insulin synthesis but only a modest increase in insulin release. The detailed action mechanism should be investigated in the next study.

In native and tumoral insulin-producing pancreatic β-cells, gap-junction protein Cx43 has been identified. Furthermore, the stable transfection of the gene coding for Cx43 induces the expression of functional gap-junction channels and improves both the biosynthetic and secretory defects of the cells. Cx43-transfection and incidence of junctional coupling also secrete more insulin than wild-type and noncommunicating cells, the absence of Cx43 implicated in the loss of β-cell-specific functions in vitro and in vivo [9,14]. In this study, HA-coating expressing high levels of the Cx43, gap junctions, and coupling, showed the striking enhancement of the amounts of stored hormone in HIT-T15 cells and promoted the glucose-induced insulin release, indicating that adequate levels of Cx43 and coupling are required for proper insulin production. These results provide further evidence that HA-coating increases the pancreatic β-cells function by enhancing the function of Cx43-mediated GJIC.

5. Conclusion

In conclusion, the function of GJIC is considered to be a useful marker for evaluating tissue-engineered products. The data obtained in this study show that gap junctions contribute to regulating some still-unknown mechanism to couple the stimulus-secretion of HIT-T15 cells under the condition of low concentration HA-coating. The growth regulation with a bioartificial pancreatic construct using HA is achievable. These results give useful information on design biocompatibility of HA when the HA is used as a biomaterial for bioartificial pancreas. HA-coating may be a new technique for constructing three-dimensional bioartificial pancreas in tissue engineering.

Acknowledgements

This work was supported in part by a Grant-in-Aid for Scientific Research on Advanced Medical Technology from Ministry of Health, Labour and Welfare, Japan and a Grant-in-Aid from Japan Human Sciences Foundations.

References

[1] Soon-Shiong P, Heintz R, Yao Q, Yao Z, Zheng T, Murphy M, et al. Insulin independence in a type I diabetic patient after encapsulated islet transplantation. Lancet 1994;343:950–1.
[2] Maki T, Monaco AP, Mullon CJP, Solomon BA. Early treatment of diabetes with porcine islets in a bioartificial pancreas. Tissue Eng 1996;2:299–306.
[3] Laurent TC, Fraser JR. Hyaluronan. FASEB J 1992;6(7):2397–404.
[4] Knudson CB, Knudson W. Hyaluronan-binding proteins in development, tissue homeostasis, and disease. FASEB J 1993;7(13):1233–41.
[5] Nagy JI, Hossain MZ, Lynn BD, Curpen GE, Yang S, Turley EA. Increased connexin-43 and gap junctional communication correlates with altered phenotypic characteristics of cells overexpressing the receptor for hyaluronic acid-mediated motility. Cell Growth Differ 1996;7(6):745–51.
[6] Park JU, Tsuchiya T. Increase in gap-junctional intercellular communications (GJIC) of normal human dermal fibroblasts

(NHDF) on surfaces coated with high-molecular-weight hyaluronic acid (HMW HA). Inc J Biomed Mater Res 2002;60(4):541–7.
[7] Meda P. The role of gap junction membrane channels in secretion and hormonal action. J Bioenergy Biomembr 1996;28(4): 369–77.
[8] Meda P, Bosco D, Chanson M, Giordano E, Vallar L, Wollheim C, et al. Rapid and reversible secretion changes during uncoupling of rat insulin-producing cells. J Clin Invest 1990;86(3): 759–68.
[9] Vozzi C, Ullrich S, Charollais A, Philippe J, Qeci L, Medz P. Adequate connexin-mediated coupling is required for proper insulin production. J Cell Biol 1995;131(6 Part 1):1561–72.
[10] Hubbell JA. Materials as morphogenetic guides in tissue engineering. Curr Opin Biotechnol 2003;14(5):551–8.
[11] Park JU, Tsuchiya T. Increase in gap junctional intercellular communications by high molecular weight hyaluronic acid associated with fibroblast growth factor 2 and keratinocyte growth factor production in normal human dermal fibroblasts. Tissue Eng 2002;8(3):419–27.
[12] Nakamura K, Yokohama S, Yoneda M, Okamoto S, Tamaki Y, Ito T, et al. High, but not low, molecular weight hyaluronan prevents T-cell-mediated liver injury by reducing proinflammatory cytokines in mice. J Gastroenterol 2004;39(4):346–54.
[13] Forrester JV, Balazs EA. Inhibition of phagocytosis by high molecular weight hyaluronate. Immunology 1980;40(3):435–46.
[14] Meda P, Chanson M, Pepper M. In vivo modulation of connexin-43 gene expression and junctional coupling of pancreatic β-cells. Exp Cell Res 1991;192(2):469–80.
[15] Charollais A, Gjinovci A, Huarte J, Bauquis J, Nadal A, Martin F, et al. Junctional communication of pancreatic beta cells contributes to control of insulin secretion and glucose tolerance. J Clin Invest 2000;106:235–43.
[16] Meda P, Pepper MS, Traub O. Differential expression of gap junction connexins in endocrine and exocrine glands. Endocrinology 1993; 133(5):2371–8.
[17] Charollais A, Serre V, Mock C, Cogne F, Bosco D, Meda P. Loss of α_1 connexin does not alter the prenatal differentiation of pancreatic β-cells and leads to the identification of another islet cell connexin. Dev Genet 1999;24(1–2):13–26.
[18] Barton W, Cristina A, Isabelle B, Melissa KL, Christopher JR. Glucose-induced translational control of proinsulin biosynthesis is proportional to preproinsulin mRNA levels in islet β-cells but not regulated via a positive feedback of secreted insulin. J Biol Chem 2003;278(43):42080–90.
[19] Lim F, Sun AM. Microencapsulated islets as bioartificial endocrine pancreas. Science 1980;210:908–10.

STUDIES ON THE EFFICACY, SAFETY AND QUALITY OF THE TISSUE ENGINEERED PRODUCTS: ENHANCEMENT OF PROLIFERATION OF HUMAN MESENCHYMAL STEM CELLS BY THE NEW POLYSACCHARIDES

Saifuddin Ahmed,[1] Toshie Tsuchiya[1] and Yutaka Kariya[2]
[1]*Division of Medical Devices, National Institute of Health Sciences, 1-18-1, Kamiyoga, Setagaya ku, Tokyo 158-8501, Japan.*
[2]*Central Research Laboratories, Seikagaku Corporation, 3-1253 Tateno Higashiyama, Tokyo 207-0021, Japan.*

Abstract: Human mesenchymal stem cells (hMSCs) have the capacity to proliferate and differentiate into multiple cells etc. Polysaccharides can modulate the cell proliferation of human endothelial cell. Here, we investigated the role of different kinds of new polysaccharides to regulate the gap junctional intercellular communication (GJIC) and cell proliferation of cultured normal human dermal fibroblasts (NHDF) cells and hMSCs. The NHDF cells and hMSCs were cultured for 4 days with new polysaccharides. The cultures were then analyzed to verify the extent of GJIC by the scrape-loading dye transfer (SLDT) method, using Lucifer yellow. Alamar blue staining was performed to determine the proliferation of the cultured cells. In NHDF cells, the GJIC was significantly inhibited in cells treated with different kinds of new polysaccharides. On the contrary, in hMSCs, the GJIC was slightly inhibited in all cultured treated cells. But proliferation was enhanced in both cells with different polysaccharides, the extents of cell proliferation was stronger in hMSCs than in NHDF cells. These findings reveal that new polysaccharides seem to play an important role in hMSCs, thus provide a novel tool on tissue engineering.

Key words: GJIC, Proliferation, NHDF, hMSCs.

1. INTRODUCTION

Human mesenchymal stem cells (hMSCs) are multipotent cells have the capacity to proliferate and differentiate into bone, cartilage and adipocytes, and are useful for human cell and gene therapies [1]. Polysaccharides are macromolecules formed from many sugar units connected by glycosidic

S. Iijima and K.-I. Nishijima (eds.), Animal Cell Technology: Basic & Applied Aspects, 81–85.